

## Folded H-Stacking Polymers by Conformational Control with 2-Substituted Trimethylene Tethers

Jun-ichi Watanabe, Tohru Hoshino, Yu-suke Nakamura, Edo Sakai, and Sentaro Okamoto\*

Department of Material & Life Chemistry, Kanagawa University, 3-27-1 Rokkakubashi, Kanagawa-ku, Yokohama 221-8686, Japan

Received May 18, 2010; Revised Manuscript Received July 11, 2010

**ABSTRACT:** Oligomers and polymers of type  $[-\text{CH}_2\text{CHRCH}_2-(\pi)-]_n$  comprising aryl units tethered by 2-substituted trimethylene were found to exist as a folding H-stacking structure in polar solvents such as  $\text{CH}_3\text{CN}$  and in film, which was evidenced by their blue-shifted UV absorption compared to that of the parent aryl compounds, and exhibited predominantly excimer-like emission. In addition, annealing of the films resulted in a unique layered structure, which may arise from the folded polymer form.

### Introduction

Controlled spatial arrangement of planar  $\pi$ -conjugate groups or molecules is of great importance in organic material development. Spatial interaction between  $\pi$ -conjugate moieties affects their photophysical, electronic and electrochemical properties such as excimer emission and charge transfer in solution or in the solid state. Their ordered assembly involving two-dimensional orientation (J- and H-aggregations) and higher dimensional assembly of  $\pi$  molecules enables us to obtain the desired properties. In this context, molecular design and synthesis for ordering fabrication modulated by molecular crystalline properties, self-assembly, and supramolecular chemistry have been intensively studied;<sup>1</sup> however, control of molecular self-association behavior and orientations remains a challenge.

Two-dimensional orientation of  $\pi$  molecules, i.e., J- and H-aggregations, gives distinct photophysical, electronic and photoelectronic properties. For instance, Dautel and Moreau have prepared films comprising J- or H-aggregates of the same  $\pi$  unit and have demonstrated that the type of aggregation significantly affects the electronic properties of the material;<sup>2</sup> the film with the J-aggregates exhibited high brightness of emission and low photoconductivity suitable for OLED (organic light-emitting diode) devices, while the film with H-aggregates displayed no brightness and higher photocurrents promising for devices of photovoltaic cell.

Also ordering assemblies of  $\pi$ -moieties in polymeric molecules is of interest because of the low processing costs and the desirable mechanical properties of electronically active polymers;<sup>3</sup> in this process, folded polymers **A** and **B** including  $\pi$ -units in a chain backbone<sup>3,4</sup> and polymers **C** having  $\pi$ -units as pendants<sup>5</sup> can be designed (Figure 1). Here, we introduce a new approach for spatial orientation of chromophores in simple, linear polymer structures of type **A**,<sup>4</sup> which are folded via conformational control with 2-substituted trimethylene tethering moieties.

### Results and Discussion

**1. Design of 2-Substituted Trimethylene Tethering Group.** First, to design the folding  $\pi$ -stacking polymer, we carried out conformational analysis of 2-substituted trimethylene-tethered<sup>6</sup> biaryl

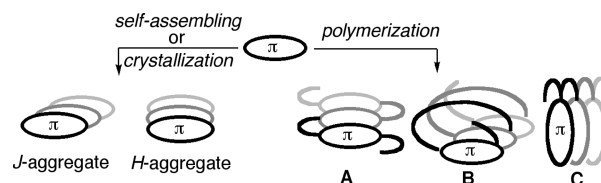
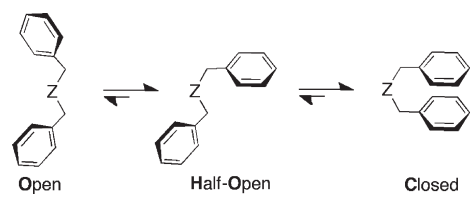


Figure 1. Ordering orientation of planar  $\pi$ -molecules (or -moieties).

derivatives **1** by molecular mechanics calculation (MM2) and by the NMR and fluorescence measurements of the corresponding synthetic samples. The results are summarized in Table 1. The table illustrates three conformations [open (**O**), half-open (**H-O**), and closed (**C**)], simplified for each 2-substituted 1,3-diphenylpropane derivative **1**, based on the energy differences calculated by molecular mechanics (MM2) (the effect of solvent was not considered). The populations of these conformations (**O:H-O:C**) at 300 K were estimated according to a Boltzmann distribution. Although the ultraviolet (UV) absorption spectra of synthetic 1,3-diphenylpropanes **1a–h** did not have remarkable difference, their emission showed distinct behavior (vide infra). The fluorescence (FL) spectra showed emission peaks at 285 and 333 nm, which may be considered as emissions from single benzene rings and benzene excimers, respectively.<sup>6</sup> The ratio of the intensities of these peaks, which were calculated by using a height of each peak, is summarized in Table 1, and the representative fluorescence spectra are shown in Figure 2.

The results of the calculation suggest that a closed (stacked) structure is a superior conformation for compounds **1b–f**; in fact, these compounds predominantly exhibited excimer-type emissions (Figure 2 and SI: S-06). For instance, **1c**, **1d**, and **1f** have the  $\lambda_{\text{em,max}}$  around 330 nm in a region of benzene excimer emission with much weaker emission from a single benzene ring (around 285 nm) (Figure 2a). Meanwhile, the calculation results suggest that the open and half-open conformations were major for 2,2-disubstituted trimethylene-tethered compound **1a**, and indeed, **1a** emitted more strongly at 280 nm than at 330 nm (Figure 2a). The steric effect of the substituent at the 2-position of the trimethylene tether was observed. Emission from single benzene ring ( $\sim 285$  nm) decreased in order of bulkiness of the 2-substituent (Figure 2b). Thus, an increase in substituent bulkiness enhanced the presence of the stacked conformation.

\*Corresponding author. E-mail: okamos10@kanagawa-u.ac.jp.

**Table 1. Conformational Analysis and Fluorescent (FL) and <sup>1</sup>H NMR Data of 2-Substituted 1,3-Diphenylpropanes 1**


<b>1</b>	Z	Distribution <sup>a</sup> O : H-O : C	Ratio of Intensities of FL at 285 and 333 nm <sup>b</sup> (excited at, nm)	δ <sup>c</sup> ppm
<b>1a</b>		48:51:1	72:28 <sup>d</sup> (259)	7.17
<b>1b</b>		2:16:82	13:87 (262)	7.05
<b>1c</b>		1:8:91	7:93 (262)	7.00
<b>1d</b>		1:9:90	1:99 (263)	6.98
<b>1e</b>		1:17:82	14:86 (262)	7.02
<b>1f</b>		0:1:99	6:94 (263)	6.95
<b>1g</b>		6:30:64	37:63 (262)	7.12
<b>1h</b>		30:19:51	48:52 (260)	7.16
	toluene	-	-	7.18

<sup>a</sup>Based on energy differences calculated by MM2 (Quantum CAChe 4.9), estimated according to a Boltzmann distribution at 300 K. <sup>b</sup>Fluorescence of a 10<sup>-4</sup> M solution in CH<sub>2</sub>Cl<sub>2</sub> at room temperature. <sup>c</sup><sup>1</sup>H NMR (CDCl<sub>3</sub>, 500 MHz, 20 °C) chemical shift of *o*-protons of Ph moieties. <sup>d</sup>Ratio of FL intensity at 282 and 333 nm.

<sup>1</sup>H NMR analyses of **1** (500 MHz, CDCl<sub>3</sub>) also supported the stability of the closed conformation for compounds **1b–g** (Table 1 and Figure 3a). In comparison to toluene spectra, compounds **1b–g** displayed an upfield shift of proton peaks at the *ortho*-position of Ph moieties in the range of 0.13–0.23 ppm because of a shielding effect along with the stacking structure. Although MM2 calculation (nonsolvent conditions), fluorescence (in CH<sub>2</sub>Cl<sub>2</sub>), and NMR (in CDCl<sub>3</sub>) measurements were conducted under different conditions, it is noteworthy that a plot of the intensity of excimer emission to the chemical shifts (○) shown in Figure 3b is in very good agreement with a plot of the calculated population of closed form to the chemical shifts (◆). Regarding *m*- and *p*-protons, similar relations were observed (SI: S-04). Figure 3c,d shows the calculated closed structure of **1d** by MM2, in which two benzene rings are nearly parallel and the distances of C1–C1' and C4–C4' were estimated to be 2.93 and 3.66 Å, respectively.

**2. Synthesis of Polymers 4 with 2-Substituted Trimethylene Tethers.** With these results, we designed polymers **4** having a 2-substituted 1,3-diphenylpropane tether of type of **1d**, expecting folded H-stacking structure **A** for the resulting polymers (Scheme 1). 1,3-Diphenylpropane tether unit **2** was readily prepared in a high yield from diethyl malonate through four steps involving dialkylation, decarboxylation, formation of tertiary alcohol, and silylation reactions. With use of the resulting tether unit **2**, both polymers **4a** [ $\pi = 2,2'$ -bithiophen-5,5'-diyl,  $M_n = 7.03 \times 10^3$ ,  $M_w/M_n = 1.44$ ,

determined by gel-permeation chromatography (GPC) analysis (eluent: THF; calibration: polystyrene standards)] and **4b** [ $\pi = (E,E)\text{-CH=CH-C}_6\text{H}_4\text{-CH=CH}$ ,  $M_n = 7.14 \times 10^3$ ,  $M_w/M_n = 1.68$ ] were synthesized by the Suzuki–Miyaura coupling reaction<sup>7</sup> with bis(boronic ester)s **3**<sup>8</sup> as a polymerization reaction. The polymers were obtained by reprecipitation from CHCl<sub>3</sub> by addition of ethyl acetate (for **4a**) or methanol (for **4b**), and their GPC analysis showed unimodal fraction profiles (SI: S-02, S-03). The reaction of **2** and **3a** in the absence of (*n*-Oct)<sub>3</sub>MeNCl resulted in the formation of the shorter polymer **4a'** ( $M_n = 2.08 \times 10^3$ ,  $M_w/M_n = 1.33$ ). Although these  $M_n$  and  $M_w$  were estimated by GPC analyses with calculation against polystyrene standards, the synthesized polymers **4** and flexible polystyrene may be much different in hydrodynamic volume, in particular if **4** would present in a folded structure. Therefore, the actual number-average molecular weights of polymers **4** may be higher than those by GPC, although, unfortunately, end-group analysis of these polymers could not be carried out due to their undefined terminal structure.

To compare the photophysical properties of polymers **4** with those of the corresponding single  $\pi$  unit, model compounds 5,5'-bis(4-methylphenyl)-2,2'-bithiophene (**diMe-P2T**)<sup>9</sup> and 1,4-bis(4-methylstyryl)benzene (**BStB**)<sup>10</sup> were prepared by the Pd-catalyzed coupling reaction of **3a** or **3b**, respectively, with 4-iodotoluene.

**3. Optical Properties of Polymers 4.** In general, the molecular aggregates in the solid state show distinct changes in

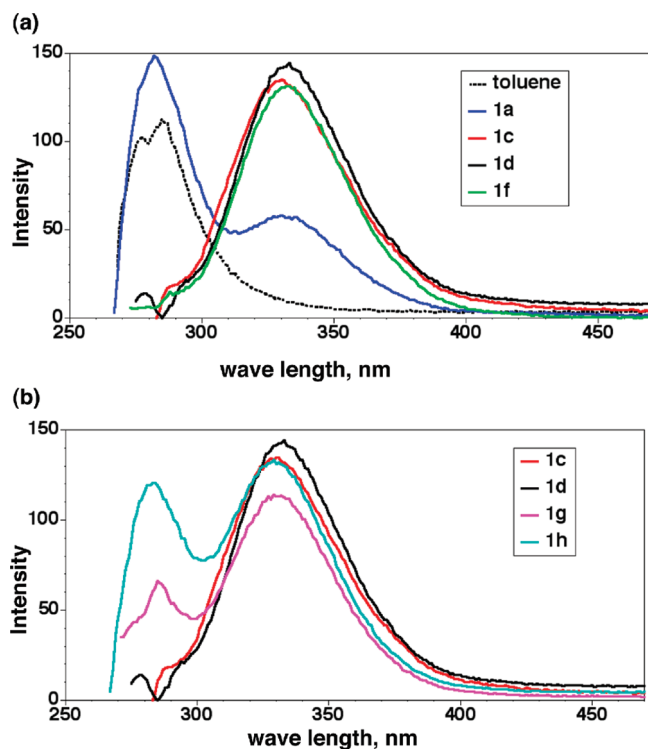


**Figure 2.** Representative fluorescence spectra of a  $\text{CH}_2\text{Cl}_2$  solution of **1** (excited at 260 or 262 nm): (a) **1a** (blue:  $10^{-4}$  M), **1c** (red:  $10^{-4}$  M), **1d** (black:  $10^{-4}$  M), **1f** (green:  $10^{-4}$  M), toluene (dotted:  $2 \times 10^{-5}$  M). (b) **1c** (red:  $10^{-4}$  M), **1d** (black:  $10^{-4}$  M), **1g** (pink:  $10^{-4}$  M), **1h** (aqua:  $10^{-4}$  M).

their absorption band as compared to their monomeric state (Figure 1). J-aggregates by a head-to-tail arrangement of the  $\pi$ -molecules display the bathochromically shifted J-bands, whereas a sandwich-type arrangement (H-aggregates) by a plane-to-plane stacking exhibits the hypsochromically shifted H-bands and also much weaker, quenched fluorescence spectra.<sup>11</sup> Therefore, to determine the orientation of  $\pi$  moieties in the synthesized polymers, ultraviolet–visible (UV–vis) absorption, fluorescence, and excitation spectra of polymers **4a**, **4a'**, and **4b** thus prepared were measured, and the results are shown in Figures 4 and 5. The concentrations (M) of polymer solutions in the figures are indicated as an amount (mol) of the repeat unit for the polymer per a volume of solution (L). The film was prepared simply by applying a  $\text{CH}_2\text{Cl}_2$  solution of polymers to quartz glass and removing the solvent, where a thickness of the film was not determined. The UV absorptions of solutions of **4a**, **4a'**, and **4b** at different concentrations were measured (SI: S-08, S-11, S-13). The results that the intensity of absorbance was proportional to the concentration in a range of  $10^{-6}$ – $10^{-4}$  M suggested that the effect of polymer aggregation in a solution on optical properties can be excluded at  $\leq 10^{-4}$  M.

In a  $\text{CH}_2\text{Cl}_2$  solution, a small blue shift (9 nm) of the absorption maximum ( $\lambda_{\text{abs,max}}$ ) of **4a** ( $\lambda_{\text{abs,max}} = 367$  nm) from that of **diMe-P2T** ( $\lambda_{\text{abs,max}} = 376$  nm) was observed, and a  $\text{CH}_3\text{CN}$  solution ( $\lambda_{\text{abs,max}} = 340$  nm) and film ( $\lambda_{\text{abs,max}} = 344$  nm) of **4a** exhibited a large blue shift from that of **diMe-P2T** (Figure 4a). Similarly, excitation spectra of **4a** ( $\lambda_{\text{ex,max}} = 336$  nm) for an emission maximum ( $\lambda_{\text{em,max}} = 512$  nm) showed a significant blue shift (38 nm) compared with that of **diMe-P2T** ( $\lambda_{\text{ex,max}} = 374$  nm for  $\lambda_{\text{em,max}} = 463$  nm), and the excitation spectra were much weaker than that of **diMe-P2T** at the same concentration (considering the repeat unit for the polymer) (Figure 4c). As revealed from normalized

fluorescence spectra of **4a** shown in Figure 4b, **4a** in  $\text{CH}_2\text{Cl}_2$  showed a broad red-shifted emission to **diMe-P2T**. A  $\text{CH}_3\text{CN}$  solution and film of **4a** exhibited similar spectra, only emitting in the excimer emission region ( $\lambda_{\text{em,max}} = 512$  nm). The emission intensity of the solutions was decreased along with their red shift at the same concentration (considering the repeat unit for the polymer) (Figure 4c). The shorter polymer (oligomer) **4a'** showed a similar but moderate photophysical trend. These results clearly demonstrate that  $\pi$ -units,  $p\text{-C}_6\text{H}_4\text{-Th-Th-}p\text{-C}_6\text{H}_4$ , in polymers **4a** were successfully assembled into the H-type stacking form in a  $\text{CH}_3\text{CN}$  solution and in film.<sup>12</sup> In contrast to these results on polymer **4a**, it has been reported that a solution of 5,5'-diphenyl-2,2'-bithiophene (**P2T**) shows 376 nm of  $\lambda_{\text{abs,max}}$ , 433 and 455 nm of  $\lambda_{\text{em,max}}$ , and 376 nm of  $\lambda_{\text{ex,max}}$  in its UV absorption, fluorescence, and excitation spectra, respectively, and its aggregate in thin film exhibits red-shifted absorption and emission ( $\lambda_{\text{abs,max}} = 440$  nm,  $\lambda_{\text{em,max}} = 515, 550$  nm).<sup>9b</sup> These indicate that **P2T** may aggregate in thin film with an orientation(s) other than that involving H-type stacking form.

Similarly, broad blue-shifted excitation and broad red-shifted emission spectra were recorded for a film of polymer **4b** compared with those of the parent  $\pi$ -unit **BStB**, where an emission was again observed predominantly in the excimer region (Figure 5). The results again demonstrate that  $\pi$ -units,  $p\text{-C}_6\text{H}_4\text{-CH=CH-}p\text{-C}_6\text{H}_4\text{-CH=CH-}p\text{-C}_6\text{H}_4$ , in polymers **4b** were assembled into the H-type stacking form in a  $\text{CH}_3\text{CN}$  solution and in film.<sup>12</sup> Thus, a blue-shifted UV-absorption against that of **BStB** was recorded for a solution of **4b** in  $\text{CH}_3\text{CN}$  (Figure 5a). Red-shifted fluorescence against **BStB** was observed for a  $\text{CH}_3\text{CN}$  solution and film of **4b** with 10 and 52 nm differences, respectively (Figure 5b). As revealed from Figure 5b, excitation spectra for these maximum emissions of **4b** in a  $\text{CH}_3\text{CN}$  solution and in film were shifted with 38 and 45 nm differences to higher energy region, respectively. It has been reported that 1,4-bis(styryl)benzene ( $\text{Ph-CH=CH-}p\text{-C}_6\text{H}_4\text{-CH=CH-Ph}$ ) are arranged layer by layer in the herringbone structure involving the H-type stacking orientation of the molecules in crystalline, and its neat film exhibits blue-shifted absorption ( $\sim 300$  nm) and red-shifted emission (460 and 488 nm) against those of the solution.<sup>10b</sup> The films of **4b** and the known 1,4-bis(styryl)benzene closely resemble each other in their spectra.

In conclusion, the spectroscopic behavior observed for a solution and film of **4a** and **4b** (blue-shifted absorption, red-shifted and quenched emission) can be attributed to their H-stacking structure. Regarding solvent effects, it can be explained that, in solution of relatively less polar solvents such as cyclohexane and  $\text{CH}_2\text{Cl}_2$ , the solvation to both less-polar polymers may disturb their ordering arrangement to make the array of  $\pi$  units irregular, whereas the polymer chain can be packed down intramolecularly in polar solvents such as  $\text{CH}_3\text{CN}$  and in film.

**4. Thermal Analyses and Morphology of Polymers 4 in Film.** From a thermogravimetry (TG) curve of polymer **4a** [SI: S-27a(b)], 5% and 10% weight loss were observed at 261 and 268 °C, respectively, where two phases of decomposition occurred. A constant weight loss (24%) observed at a range of 300–400 °C could be considered as decomposition by elimination of silanol ( $\text{HOSiEt}_3$ ) from the silyl ether structure of tertiary alcohol in the polymer, since  $\text{HOSiEt}_3$  is 24 wt % in the repeat unit structure for the polymer. Similar phenomena were recorded for polymer **4b** (SI: S-27b).

On the basis of the results of TG analysis of **4a**, two peaks at 192 °C and around 260 °C observed in differential thermal analysis (DTA) [SI: S-27a(a)] may be assigned to be for melting and decomposition by the elimination of silanol,

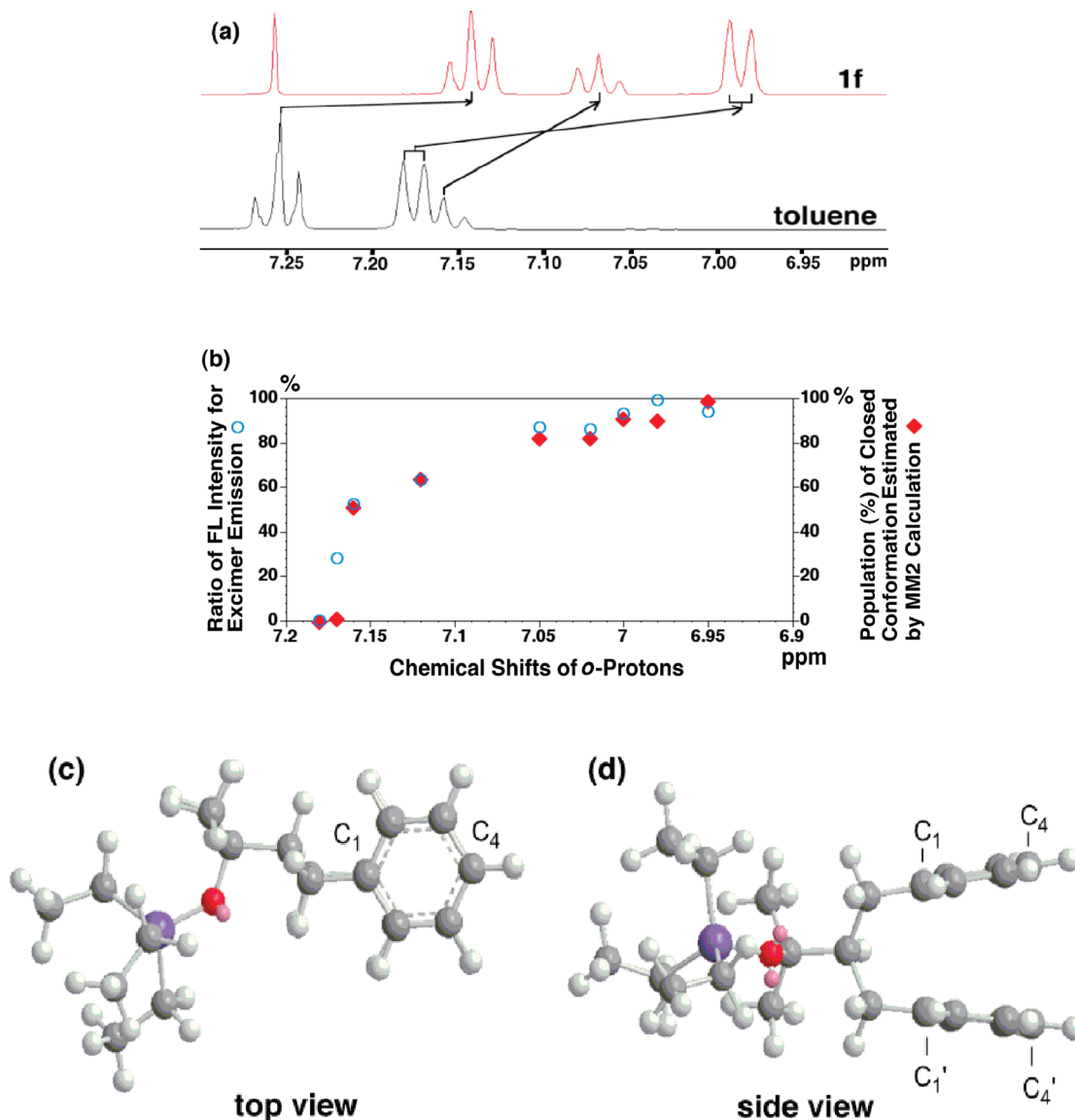


**Figure 3.** (a) <sup>1</sup>H NMR spectra of **1f** and toluene (CDCl<sub>3</sub>, 500 MHz, 20 °C). (b) Relation between chemical shifts of *o*-protons of **1** and distribution of the closed conformation estimated by fluorescence (○) or MM2 calculation (◆). (c) Top view and (d) side view of the MM2-optimized structure for **1d** (gray: C; red: O; purple: Si).

respectively. The DTA chart of **4b** and optical microscopic observation suggested that the melting started around 210 °C, the temperature of which was close to the temperature for beginning decomposition (~230 °C) (SI: S-27b).

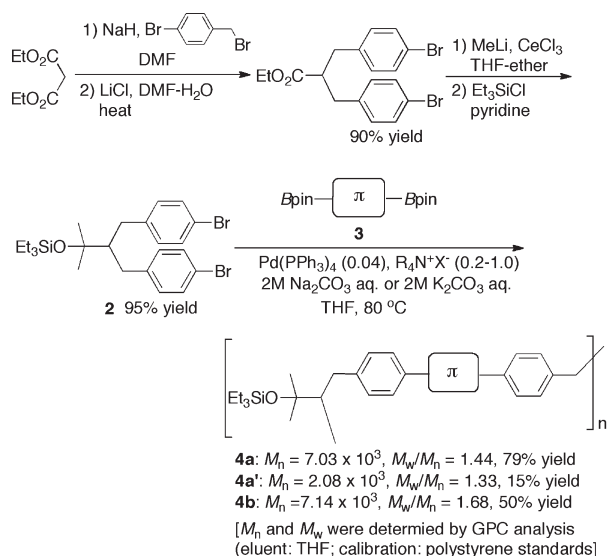
The differential scanning calorimetry (DSC) profile for the first heating of **4a** to 220 °C (10 °C/min) showed three peaks, which can respectively be considered as temperatures for glass transition (115.5 °C), crystallization (around 144 °C), and melting (around 180 °C) (SI: S-28a). But in the chart for a second heating, the peaks became less clear and the third heating exhibited only a peak around 125 °C. The DSC profiles obtained for polymer **4b** had a similar trend (SI: S-28b). Although rationalization of the behavior of enthalpy changes for these peculiar polymers is unclear at this time and must await further study, based on these DTA, TG, and DSC data along with optical microscopic observation, we set an annealing procedure of films of **4a** and **4b** (vide infra).

A film of polymer **4a**, which was prepared by spin-coating on a silicon substrate through the use of its CH<sub>2</sub>Cl<sub>2</sub> solution and solvent removal, provided only a flat surface image in atomic force microscope (AFM) analysis. However, an

interesting AFM images were obtained after annealing (heated to melt at 210 °C for 1 min, cooled to 160 °C for 2 min and then to rt) (Figure 6a). The observed film surface had craterlike holes that displayed an inner layered structure of the film. Each of the layers had a thickness of 3 nm, the length of which is in good agreement with that calculated for the width of the expected folded structure of polymer **4a** as illustrated in Figure 7.

X-ray diffraction (XRD) analyses of polymer powder peeled from the film, prepared by spin-coating on a silicon substrate and removing the solvent, were carried out for the samples before and after annealing treatment mentioned above (Figure 6b,c). Observed XRD patterns were nearly identical before and after annealing, and both showed a sharp peak at 2.96 nm, the length of which is again in good agreement with the calculated width of the expected folded structure of **4a** (Figure 7). A polymer powder just after precipitation from the CHCl<sub>3</sub> solution also showed almost the same reflection profile (data not shown). From these observations, we assume that a polymer molecule of **4a** may have an ordered aggregate morphology with its folded

Scheme 1



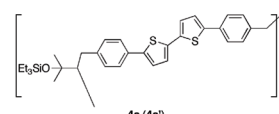
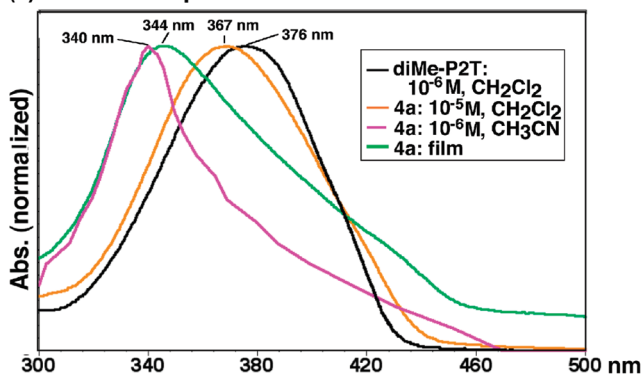
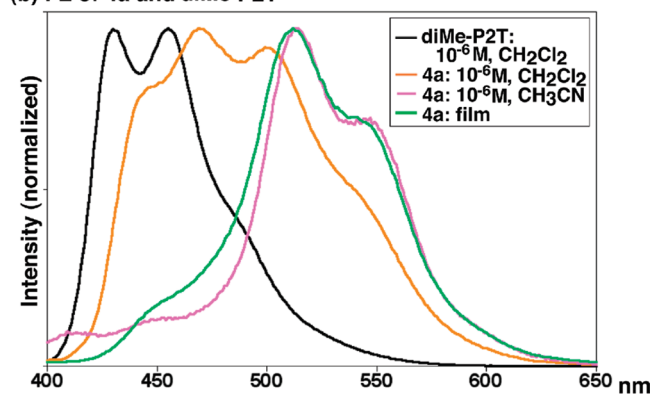
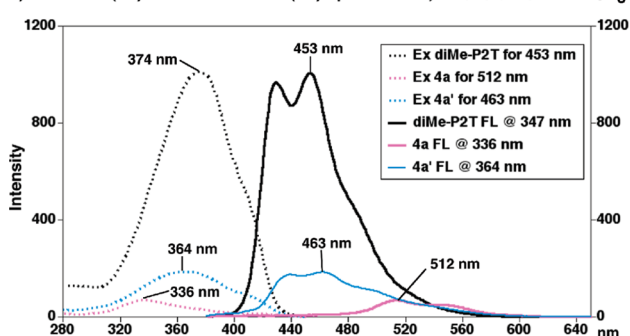
structure in the solid state of precipitates and cast-film, and then annealing of this film produces a layered structure as illustrated in Figure 7. Similarly, the XRD profile for an annealed film of polymer **4b** had a sharp peak of 3.02 nm (Figure 6d), the value of which is somewhat larger than that of **4a**. It is in good agreement with the fact that a  $\pi$ -unit of **4b**, bis(styryl)benzene, is  $\sim 1$  Å longer than that of **4a**, diphenylbithiophene (Figure 7). The assignment of other peaks observed by XRD analyses must await further study.

## Conclusion

We have demonstrated that, in simple linear skipped  $\pi$  polymers, conformational control via 2-substituted trimethylene tethering groups makes the polymer fold, which stabilizes the H-type stacking form in solution as well as in solids. The XRD patterns of the pristine film before annealing and the annealed film of **4a** were nearly identical, both of which had a sharp peak at 3 nm, nearly identical to the width of the expected folded polymer structures. Thus, we have synthesized and designed a new polymer programmed to fold in H-stacking. This may be important for charge transport as requested on solar cell. In addition, we have also obtained nanostructured morphologies by annealing the films while keeping the layered structure, the nanostructure of which may be also of importance as requested on photovoltaic cell. The present approach for controlling the spatial arrangement might be expected to become a novel motif for the development of new soft materials, and further investigation on the possible application by changing the structure of  $\pi$  unit included is underway.

## Experimental Section

**General Data.** NMR spectra were recorded in  $\text{CDCl}_3$  at 600, 500, 270, and 90 MHz for  $^1\text{H}$  and 150, 125, 67.5, and 22.5 MHz

(a) UV-Vis absorption of **4a** and diMe-P2T(b) FL of **4a** and diMe-P2T(c) Excitation (Ex) and Fluorescence (FL) Spectra of **4a**, **4a'** and diMe-P2T in  $\text{CH}_3\text{CN}$ 

**Figure 4.** UV-vis absorption and fluorescence spectra of polymer **4a** and oligomer **4a'**: (a) UV-vis absorption (normalized):  $10^{-6}$  M for diMe-P2T (black),  $10^{-5}$  M for **4a** in  $\text{CH}_2\text{Cl}_2$  (orange),  $10^{-5}$  M for **4a** in  $\text{CH}_3\text{CN}$  (pink), and film of **4a** (green). (b) Fluorescence (normalized):  $10^{-6}$  M. Excited at 375 nm for diMe-P2T (black), 367 nm for **4a** in  $\text{CH}_2\text{Cl}_2$  (orange), 336 nm for **4a** in  $\text{CH}_3\text{CN}$  (pink), and 344 nm for a film of **4a** (green). (c) Fluorescence:  $10^{-6}$  M solution in  $\text{CH}_3\text{CN}$ , excited at 374 nm for diMe-P2T (black), 336 nm for **4a** (pink), and 364 nm for **4a'** (blue).

for  $^{13}\text{C}$ , respectively, on JEOL JNM-ECA600, 500 and -EX270 and HITACHI R-1900 spectrometers. Chemical shifts are reported in parts per million (ppm,  $\delta$ ) relative to  $\text{Me}_4\text{Si}$  ( $\delta$  0.00), residual  $\text{CHCl}_3$  ( $\delta$  7.26 for  $^1\text{H}$  NMR), or a center peak of  $\text{CDCl}_3$  ( $\delta$  77.0 for  $^{13}\text{C}$  NMR). IR spectra were recorded on an FT-IR spectrometer (JASCO FT/IR-4100). All reactions sensitive to oxygen and/or moisture were performed under an argon atmosphere. The  $M_n$  and  $M_w/M_n$  of polymers were measured with a TOSOH HLC-8020 gel-permeation chromatography (GPC)

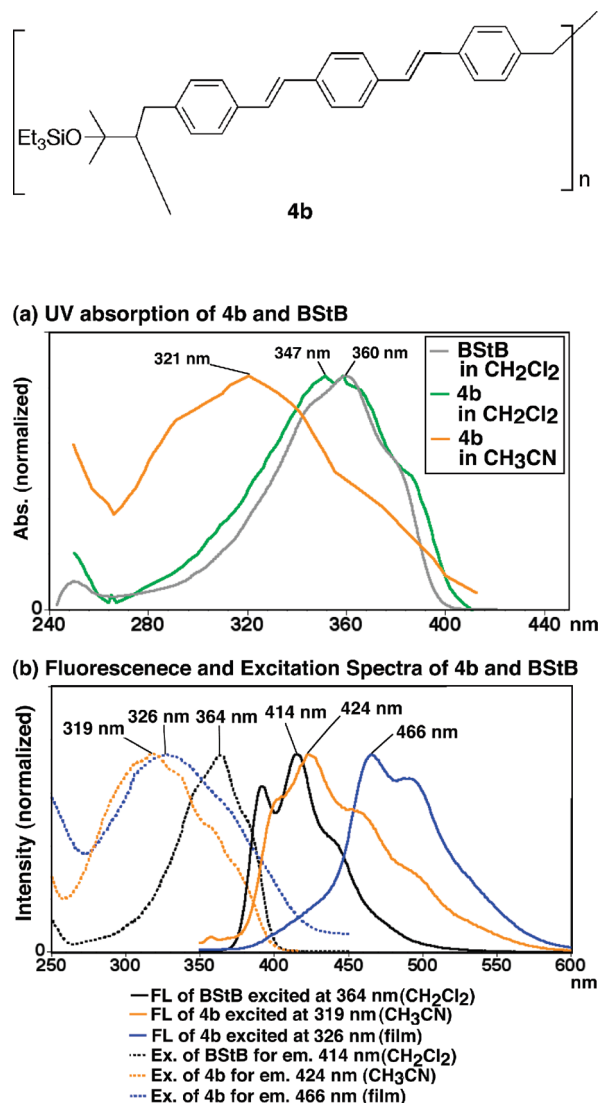


**Figure 5.** UV absorption, fluorescence, and excitation spectra of polymer **4b** and **BStB**. (a) UV absorption: **BStB** (gray,  $10^{-7}$  M in  $\text{CH}_2\text{Cl}_2$ ), **4b** (green,  $10^{-6}$  M in  $\text{CH}_2\text{Cl}_2$ ), **4b** (peach,  $10^{-6}$  M in  $\text{CH}_3\text{CN}$ ). (b) Fluorescence: **BStB** (black,  $10^{-7}$  M in  $\text{CH}_2\text{Cl}_2$ ), **4b** (peach,  $10^{-6}$  M in  $\text{CH}_3\text{CN}$ ), **4b** (blue, film). Excitation: **BStB** (black,  $10^{-7}$  M in  $\text{CH}_2\text{Cl}_2$ ), **4b** (peach,  $10^{-6}$  M in  $\text{CH}_3\text{CN}$ ), **4b** (blue, film).

unit (eluent: THF; calibration: polystyrene standards) using two TSK-gel columns ( $2 \times$  Multipore  $\text{H}_{\text{XL}}\text{-M}$ ). High-resolution mass spectra (HR-MS) were measured on JEOL Accu TOF T-100 equipped with ESI ionization. UV-vis absorption spectra were recorded on a Shimadzu UV-2450 spectrometer. Excitation and fluorescence spectra were measured on a Shimadzu RF-5300PC spectrometer. Thermogravimetry/differential thermal analysis (TG/DTA) was carried out with Seiko Instruments Inc. EXSTAR6000 TG/DTA6200 under nitrogen (heating rate:  $10^\circ\text{C}/\text{min}$ ). Differential scanning calorimetry (DSC) measurement was carried out with Seiko Instruments Inc. EXSTAR6000 DSC6220 under nitrogen (heating rate:  $10/\text{min}$ ; cooling rate:  $5^\circ\text{C}/\text{min}$ ). AFM images were recorded under ambient conditions using a Digital Instrument Nanoscope V operating in the tapping mode. X-ray diffraction (XRD) patterns were obtained using a Rigaku RINT-UltimaIII diffractometer with  $\text{Cu K}\alpha$  radiation. Molecular mechanics (MM2) calculations were performed using Quantum CACHE 4.9 program package. On the basis of the energy differences calculated by MM2, the populations of these conformations (O:H-O:C) were estimated according to a Boltzmann distribution. 1,3-Diphenylpropane

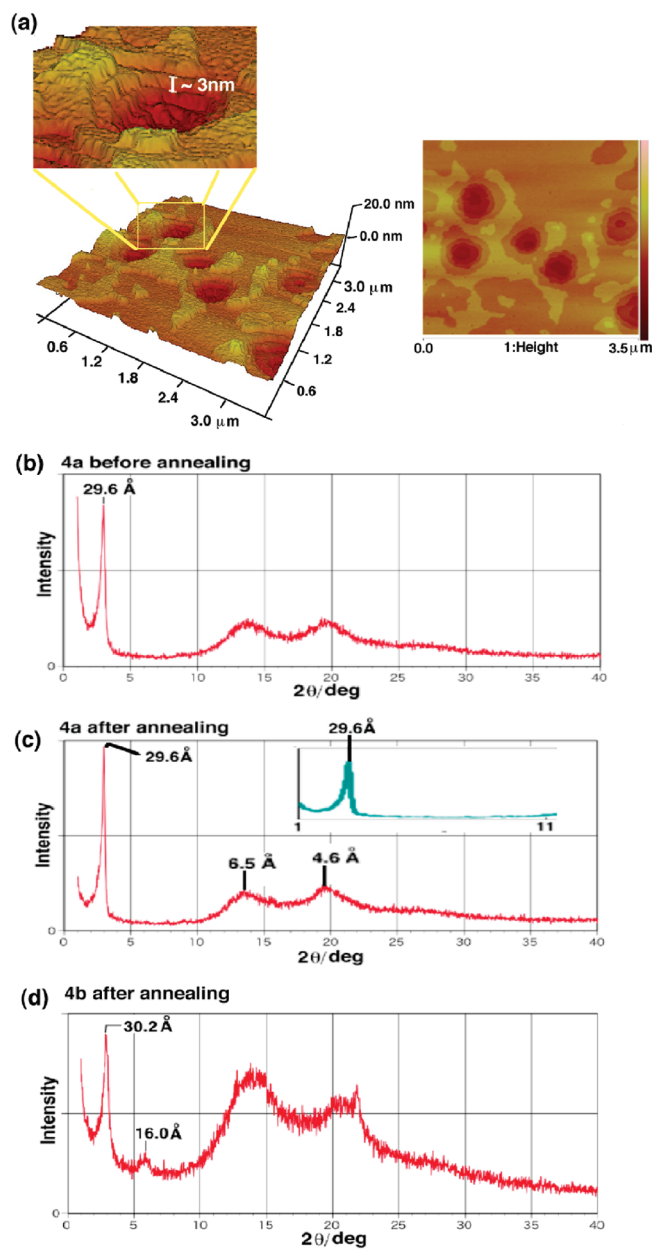


**Figure 6.** AFM images and XRD spectrum of **4a** and **4b**. (a) AFM images of **4a** film (spin-coated on silicon substrate, heated at  $210^\circ\text{C}$  for 1 min, cooled to  $160^\circ\text{C}$  for 2 min, and then cooled to rt). (b) XRD chart of **4a** (after spin-coating and removing solvent and before annealing, film was removed from the substrate, and the resulting powder was analyzed). (c) XRD chart of **4a** (after annealing on a silicon substrate, film was removed from the substrate, and the resulting powder was analyzed). (d) XRD chart of **4b** (after annealing on a silicon substrate, film was removed from the substrate, and the resulting powder was analyzed).

derivatives **1b-h** were prepared from **1a**, which was obtained by the reaction of diethyl malonate and benzyl bromide with NaH in DMF, by the conventional reactions according to the procedure (see SI: S-01). Dry solvents (THF and ether) were purchased from Kanto Chemical Co., Inc., and used as received without any additional purification and degassing procedure. The structures of synthesized **diMe-P2T**<sup>9</sup> and **BStB**<sup>10</sup> were confirmed by comparison of their spectral data with those reported.

**Ethyl 2-(4-Bromobenzyl)-3-(4-bromophenyl)propanoate.** To a mixture of NaH (55% in oil, 2.95 g, 67.5 mmol) and DMF (60 mL) was added diethyl malonate (4.53 mL, 30.0 mmol) at  $0^\circ\text{C}$ . After being stirred for 30 min at  $0^\circ\text{C}$ , to the mixture was

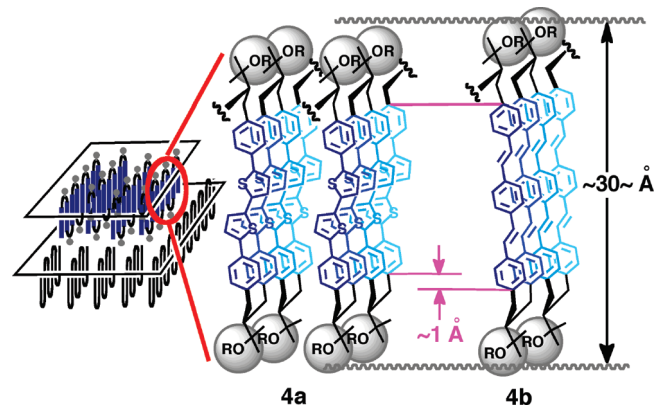


**Figure 7.** Illustration of postulated layer structure for annealed films of **4a** and **4b**.

added 4-bromobenzyl bromide (15.7 g, 63.0 mmol), and the reaction mixture was stirred for 2 h at room temperature. After checking completion of the reaction by TLC analysis, the mixture was quenched with saturated aqueous  $\text{NH}_4\text{Cl}$ , and the aqueous layer was extracted with AcOEt. The combined organic layers were washed with brine, dried over anhydrous  $\text{MgSO}_4$ , filtered through a pad of Celite, and concentrated in vacuo. To the resulting residue were added  $\text{LiCl}$  (5.09 g, 120 mmol),  $\text{H}_2\text{O}$  (1.08 mL, 60.0 mmol), and DMF (100 mL) at room temperature, and the reaction mixture was stirred for 7 h at 160 °C. After checking completion of the reaction by TLC analysis, the mixture was quenched with water, and the aqueous layer was extracted with AcOEt. The organic layers were washed with brine, dried over anhydrous  $\text{MgSO}_4$ , filtered through a pad of Celite, and concentrated in vacuo. The residue was chromatographed on silica gel (hexane:AcOEt = 30:1) to give ethyl 2-(4-bromobenzyl)-3-(4-bromophenyl)propanoate (11.5 g, 27.0 mmol) in 90% yield as a yellow oil.  $^1\text{H}$  NMR (600 MHz,  $\text{CDCl}_3$ )  $\delta$  7.39 (d, 4H,  $J = 8.4$  Hz, Ar), 7.02 (d, 4H,  $J = 7.8$  Hz, Ar), 3.96 (q, 2H,  $J = 7.4$  Hz,  $\text{CO}_2\text{CH}_2\text{CH}_3$ ), 2.92–2.85 (m, 3H,  $\text{CHCH}_2\text{Ar}$  and  $\text{CHCH}_2\text{Ar}$ ), 2.73 (dd, 2H,  $J = 4.8$ , 12.6 Hz,  $\text{CH}_2\text{Ar}$ ), 1.03 (t, 3H,  $J = 7.2$  Hz,  $\text{CO}_2\text{CH}_2\text{CH}_3$ ).  $^{13}\text{C}$  NMR (150 MHz,  $\text{CDCl}_3$ ):  $\delta$  174.3, 137.8, 131.5, 130.6, 120.4, 60.5, 49.2, 37.6, 14.0. IR (neat): 2962, 1731, 1592, 1488, 1445, 1405, 1375, 1259, 1214, 1160, 1103, 1072, 1012, 806.1  $\text{cm}^{-1}$ . HR-MS:  $m/z = \text{calcd for } \text{C}_{18}\text{H}_{18}\text{Br}_2\text{NaO}_2 [\text{M} + \text{Na}]^+$ : 446.9571; found 446.9586.

**(3-(4-Bromobenzyl)-4-(4-bromophenyl)-2-methylbutan-2-yloxy)-triethylsilane (2).** To a mixture of  $\text{CeCl}_3$  (4.44 g, 18.0 mmol) and THF (48 mL) which had been stirred for 12 h at room temperature was added MeLi (in  $\text{Et}_2\text{O}$  1.6 M, 11.3 mL, 18.0 mmol) at  $-78$  °C. After being stirred for 1 h at  $-78$  °C, to the mixture was added a solution of ethyl 2-(4-bromobenzyl)-3-(4-bromophenyl)propanoate (2.56 g, 6.00 mmol) in THF (6.0 mL), and the reaction mixture was stirred for 2 h at  $-78$  °C. After checking completion of the reaction by TLC analysis, the mixture was quenched with 0.1 M aqueous  $\text{CH}_3\text{COOH}$ , and the aqueous layer was extracted with AcOEt. The combined organic layers were washed with water, dried over  $\text{Na}_2\text{SO}_4$ , filtered through a pad of Celite, and concentrated in vacuo. To the resulting residue was added pyridine (12 mL) and triethylsilyl chloride (1.3 mL, 7.5 mmol) at room temperature, and the reaction mixture was stirred for 20 h at 60 °C. After checking completion of the reaction by TLC analysis, the mixture was quenched with saturated aqueous  $\text{NH}_4\text{Cl}$ , and the aqueous layer was extracted with hexane. The combined organic layers were washed with water, dried over anhydrous  $\text{MgSO}_4$ , filtered through a pad of Celite, and concentrated in vacuo. The residue was chromatographed on silica gel (hexane only) to give **2** (3.00 g, 5.7 mmol) in 95% yield as colorless oil.  $^1\text{H}$  NMR (600 MHz,  $\text{CDCl}_3$ ):  $\delta$  7.25 (d, 4H,  $J = 8.4$  Hz, Ar), 6.81 (d, 4H,  $J = 8.4$  Hz, Ar), 2.92 (dd, 2H,  $J = 4.8$ , 14.4 Hz,  $\text{CH}_2\text{Ar}$ ), 2.30 (dd, 2H,  $J = 8.1$ , 14.1 Hz,  $\text{CH}_2\text{Ar}$ ), 2.00 (tt, 1H,  $J = 4.3$ , 8.4 Hz,  $\text{CHCH}_2\text{Ar}$ ),

1.21 (s, 6H,  $(\text{CH}_3)_2\text{C}$ ), 0.97 (t, 9H,  $J = 7.8$  Hz,  $(\text{CH}_3\text{CH}_2)_3\text{Si}$ ), 0.61 (q, 6H,  $J = 8.0$  Hz,  $(\text{CH}_3\text{CH}_2)_3\text{Si}$ ).  $^{13}\text{C}$  NMR (150 MHz,  $\text{CDCl}_3$ ):  $\delta$  141.4, 131.1, 130.6, 119.1, 76.1, 54.9, 36.2, 28.2, 7.2, 6.9. IR (neat): 2954, 2874, 1591, 1488, 1459, 1404, 1383, 1365, 1236, 1178, 1143, 1102, 1072, 1012, 798.4, 724.1  $\text{cm}^{-1}$ . HR-MS:  $m/z = \text{calcd for } \text{C}_{24}\text{H}_{34}\text{Br}_2\text{KOSi} [\text{M} + \text{K}]^+$ : 563.0383; found 563.0352.

**Polymers 4a and 4a'.** To a solution of **2** (2.11 g, 4.0 mmol), **3a** (1.67 g, 4.0 mmol), (*n*-Oct) $_3\text{MeNCl}$  (330 mg, 0.82 mmol) in 2 M aqueous  $\text{Na}_2\text{CO}_3$  (8.0 mL), and THF (22 mL) which had been deaerated for 1 h was added a solution of  $\text{Pd}(\text{PPh}_3)_4$  (185 mg, 0.16 mmol) in THF (5.0 mL). The reaction mixture was stirred for 12 h (polymer **4a'**) or 3 days (polymer **4a**) at 80 °C, and then it was cooled to room temperature. The resulting mixture was added into a saturated aqueous  $\text{NaHCO}_3$ , and the product was extracted with  $\text{CHCl}_3$  three times. The combined organic layers were washed with water and dried over anhydrous  $\text{Na}_2\text{SO}_4$ . After filtration and evaporation, the residue was dissolved in  $\text{CHCl}_3$  and poured into a large amount of MeOH. The resulting residue was dissolved in  $\text{CHCl}_3$  and poured into a large amount of AcOEt. The obtained polymer was washed with AcOEt several times and dried under reduced pressure. A brown solid polymer **4a** was obtained. **Polymer 4a.** Yield: 1.68 g, 3.16 mmol, 79%. GPC:  $M_n = 7.03 \times 10^3$ ,  $M_w = 1.01 \times 10^4$ ,  $M_w/M_n = 1.44$ .  $^1\text{H}$  NMR ( $\text{CDCl}_3$ , 600 MHz):  $\delta$  7.42–6.70 (br m, overlap with  $\text{CHCl}_3$  peak, 12H in one unit, Ar), 3.08–2.89 (br, 2H in one unit,  $\text{CH}_2\text{Ar}$ ), 2.43–2.24 (br, 2H in one unit,  $\text{CH}_2\text{Ar}$ ), 2.19–2.08 (br, 1H in one unit,  $\text{CHCH}_2\text{Ar}$ ), 1.36–1.13 (br, 6H in one unit,  $(\text{CH}_3)_2\text{C}$ ), 1.07–0.86 (br, 9H in one unit,  $(\text{CH}_3\text{CH}_2)_3\text{Si}$ ), 0.73–0.47 (br, 6H in one unit,  $(\text{CH}_3\text{CH}_2)_3\text{Si}$ ).  $^{13}\text{C}$  NMR ( $\text{CDCl}_3$ , 150 MHz):  $\delta$  142.9, 141.9, 136.2, 135.7, 131.2, 129.4, 127.7, 125.5, 125.1, 124.2, 123.2, 76.1, 54.9, 36.7, 34.2, 30.3, 29.4, 28.1, 7.3, 6.9. IR (film): 2954, 2875, 1497, 1445, 1415, 1382, 1364, 1215, 1177, 1144, 1112, 1040, 790.7, 740.5  $\text{cm}^{-1}$ . **Polymer 4a'.** Yield: 0.319 g, 0.60 mmol, 15%. GPC:  $M_n = 2.08 \times 10^3$ ,  $M_w = 2.77 \times 10^3$ ,  $M_w/M_n = 1.33$ .

**Polymer 4b.** To a solution of **2** (790 mg, 1.50 mmol), **3b** (573 mg, 1.50 mmol), (*n*-Bu) $_4\text{NBr}$  (484 mg, 1.50 mmol) in 2 M aqueous  $\text{K}_2\text{CO}_3$  (3.0 mL), and THF (8.0 mL) which had been deaerated for 1 h was added a solution of  $\text{Pd}(\text{PPh}_3)_4$  (69 mg, 0.060 mmol) in THF (2.0 mL). The reaction mixture was stirred for 3 days at 80 °C, and then it was cooled to room temperature. The resulting mixture was added into a saturated aqueous  $\text{NaHCO}_3$ , and the product was extracted with  $\text{CHCl}_3$  three times. The combined organic layers were washed with water and dried over anhydrous  $\text{Na}_2\text{SO}_4$ . After filtration and evaporation, the residue was dissolved in  $\text{CHCl}_3$  and poured into a large amount of MeOH. The obtained polymer was washed with  $\text{Et}_2\text{O}$  several times and dried under reduced pressure. The polymer **4a** (371 mg, 0.751 mmol) was obtained in 50% yield as a yellow-brown solid. GPC:  $M_n = 7.14 \times 10^3$ ,  $M_w = 1.20 \times 10^4$ ,  $M_w/M_n = 1.68$ .  $^1\text{H}$  NMR ( $\text{CDCl}_3$ , 600 MHz):  $\delta$  7.44–6.81 (br m, overlap with  $\text{CHCl}_3$  peak, 16H, Ar and  $\text{CH}=\text{CH}$ ), 3.13–2.77 (br, 2H,  $\text{CH}_2\text{Ar}$ ), 2.48–2.23 (br, 2H,  $\text{CH}_2\text{Ar}$ ), 2.16–2.00 (br, 1H,  $\text{CH}_2\text{Ar}$ ), 1.35–1.04 (br, 6H,  $(\text{CH}_3)_2\text{C}$ ), 1.04–0.83 (br, 9H,  $(\text{CH}_3\text{CH}_2)_3\text{Si}$ ), 0.71–0.48 (br, 6H,  $(\text{CH}_3\text{CH}_2)_3\text{Si}$ ).  $^{13}\text{C}$  NMR ( $\text{CDCl}_3$ , 150 MHz):  $\delta$  142.3, 136.6, 134.5, 129.3, 128.7, 128.4, 127.3, 126.7, 126.5, 126.2, 76.2, 54.9, 36.6, 28.3, 7.3, 6.9. IR (film): 3021, 2954, 2875, 1600, 1516, 1459, 1419, 1383, 1364, 1212, 1177, 1144, 1110, 1040, 960.4, 825.4, 724.1, 549.6  $\text{cm}^{-1}$ .

**Acknowledgment.** We thank the Scientific Frontier Research Project from the Ministry of Education, Culture, Sports, Science and Technology, Japan for financial support. We thank Prof. T. Ikehara and Dr. T. Kataoka, Kanagawa University for AFM analysis.

**Supporting Information Available:** Experimental and analytical details and spectroscopic data. This material is available free of charge via the Internet at <http://pubs.acs.org>.

## References and Notes

- (1) Recent reviews: (a) DiBenedetto, S. A.; Facchetti, A.; Ratner, M. A.; Marks, T. J. *Adv. Mater.* **2009**, *21*, 1407–1433. (b) Wouters, D.; Hoepfner, S.; Schubert, U. S. *Angew. Chem., Int. Ed.* **2009**, *48*, 1732–1739. (c) Hirst, A. R.; Escuder, B.; Miravet, J. F.; Smith, D. K. *Angew. Chem., Int. Ed.* **2008**, *47*, 8002–8018. (d) Yashima, E.; Maeda, K.; Iida, H.; Furusho, Y.; Nagai, K. *Chem. Rev.* **2009**, *109*, 6102–6211. (e) Cheng, Y.-J.; Yang, S.-H.; Hsu, C.-S. *Chem. Rev.* **2009**, *109*, 5868–5923. (f) Boussicault, F.; Robert, M. *Chem. Rev.* **2008**, *108*, 2622–2645. (g) Szacilowski, K. *Chem. Rev.* **2008**, *108*, 3481–3548.
- (2) Dautel, O. J.; Wantz, G.; Aimairac, R.; Flot, D.; Hirsch, L.; Lere-Porte, J.-P.; Parneix, J. P.; Serein-Spirau, F.; Vignau, L.; Moreau, J. J. E. *J. Am. Chem. Soc.* **2006**, *128*, 4892–4901.
- (3) (a) Smaldone, R. A.; Moore, J. S. *Chem.—Eur. J.* **2008**, *14*, 2650–2657. (b) *Foldamers: Structure, Properties and Applications*; Hecht, S., Huc, I., Eds.; Wiley-VCH: Weinheim, 2007. (c) Cheng, P. *Curr. Opin. Struct. Biol.* **2004**, *14*, 512–520. (d) Schmuck, C. *Angew. Chem., Int. Ed.* **2003**, *42*, 2448–2452. (e) Hill, D. J.; Mio, M. J.; Prince, R. B.; Hughes, T. S.; Moore, J. S. *Chem. Rev.* **2001**, *101*, 3893–4012. (f) Cheng, R. P.; Gellman, S. H.; DeGrado, W. F. *Chem. Rev.* **2001**, *101*, 3219–3232. (g) Nakano, T.; Okamoto, Y. *Chem. Rev.* **2001**, *101*, 4013–4038. (h) Gellman, S. H. *Acc. Chem. Res.* **1998**, *31*, 173–180.
- (4) With a rigid urea or dialkylsilylene tether, see: (a) Yamaguchi, K.; Matsumura, G.; Kagechika, H.; Azumaya, I.; Ito, Y.; Itai, A.; Shudo, K. *J. Am. Chem. Soc.* **1991**, *113*, 5474–5475. (b) Krebs, F. C.; Jorgensen, M. *J. Org. Chem.* **2002**, *67*, 7511–7518. (c) Kurth, T. L.; Lewis, F. D. *J. Am. Chem. Soc.* **2003**, *125*, 13760–13767. (d) Yeh, M.-Y.; Lin, H.-C.; Lee, S.-L.; Chen, C.-H.; Lim, T.-S.; Fann, W.; Luh, T.-Y. *Chem. Commun.* **2007**, 3459–3461. With a flexible long tether, see: (e) Wang, W.; Li, L.-S.; Heims, G.; Zhou, H.-H.; Li, A. D. G. *J. Am. Chem. Soc.* **2003**, *125*, 1120–1121. (f) Han, J. J.; Shaller, A. D.; Wang, W.; Li, A. D. Q. *J. Am. Chem. Soc.* **2008**, *130*, 6974–6982. (g) Ghosh, S.; Ramakrishnan, S. *Angew. Chem., Int. Ed.* **2004**, *43*, 3264–3268. For layered polymers, see: (h) Morisaki, Y.; Imoto, H.; Miyake, J.; Chujo, Y. *Macromol. Rapid Commun.* **2009**, *30*, 1094–1100. (i) Morisaki, Y.; Fernandes, J. A.; Chujo, Y. *Macromol. Rapid Commun.* **2009**, *30*, 2107–2111.
- (5) (a) Nakano, T.; Takewaki, K.; Yada, T.; Okamoto, Y. *J. Am. Chem. Soc.* **2001**, *123*, 9182–9183. (b) Nakano, T.; Yada, T. *J. Am. Chem. Soc.* **2003**, *125*, 15474–15484. (c) Rathore, R.; Abdelwahed, S. H.; Guzei, I. A. *J. Am. Chem. Soc.* **2003**, *125*, 8712–8713.
- (6) Hirayama, F. *J. Chem. Phys.* **1965**, *42*, 3163–3171.
- (7) (a) Koch, F.; Heitz, W. *Macromol. Chem. Phys.* **1997**, *198*, 1531–1544. (b) Schlüter, A. D. *J. Polym. Sci., Part A: Polym. Chem.* **2001**, *39*, 1533–1556.
- (8) Lee, T.; Baik, C.; Jung, I.; Song, K. H.; Kim, S.; Kim, D.; Kang, S. O.; Ko, J. *Organometallics* **2004**, *23*, 4569–4575.
- (9) (a) Hotta, S.; Lee, S. A.; Tamaki, T. *J. Heterocycl. Chem.* **2000**, *37*, 25–29. (b) Lee, S. A.; Hotta, S.; Nakashima, F. *J. Phys. Chem. A* **2000**, *104*, 1827–1833.
- (10) (a) Nakatsuji, S.; Matsuda, K.; Uesugi, Y.; Nakashima, K.; Akiyama, S.; Katzer, G.; Fabian, W. *J. Chem. Soc., Perkin Trans. 2* **1991**, 861–867. (b) Kabe, R.; Nakanotani, H.; Sakanoue, T.; Yahiro, M.; Adachi, C. *Adv. Mater.* **2009**, *21*, 4034–4038.
- (11) (a) Jelly, E. E. *Nature* **1936**, *138*, 1009–1010. (b) Scheibe, G. *Angew. Chem.* **1936**, *49*, 563. (c) Brooker, L. G. S.; White, F. L.; Heseltine, D. W.; Keyes, G. H.; Dent, S. G.; VanLare, E. J. *J. Photogr. Sci.* **1953**, *1*, 173–183. (d) McRae, E. G.; Kasha, M. *J. Chem. Phys.* **1958**, *28*, 721–722. (e) Kasha, M.; Rawls, H. R.; El-Bayoumi, M. A. *Pure Appl. Chem.* **1965**, *11*, 371–392.
- (12) (a) Brooker, L. G. S.; White, F. L.; Heseltine, D. W.; Keyes, G. H.; Dent, S. G.; VanLare, E. J. *J. Photogr. Sci.* **1953**, *1*, 173–183. (b) Davydov, A. S. *Theory of Molecular Excitons*; Plenum: New York, 1971.